Linear stability approach to explain lock-in transition and time sharing in vortex-induced vibrations of slender structures

Rémi Violette, Julien Szydlowski, Emmanuel de Langre

Proceedings of the ASME 2009 28th International Conference on Ocean, Offshore and Arctic Engineering
OMAE2009
May 31 - June 5, 2009, Honolulu, Hawaii, USA

OMAE2009-80132

LINEAR STABILITY APPROACH TO EXPLAIN LOCK-IN TRANSITION AND TIME SHARING IN VORTEX-INDUCED VIBRATIONS OF SLENDER STRUCTURES

Rémi Violette
IFP/LadHyX

Julien Szydlowski *

Département de mécanique appliquée
Institut Français du Pétrole
Rueil Malmaison, 92852, France
Julien.SZYDLOWSKI@ifp.fr

Emmanuel de Langre

Département de mécanique
LadHyX, CNRS - Ecole Polytechnique
Palaiseau, 91128, France

ABSTRACT

In this paper, we use a linearized version of a wake oscillator model in order to understand VIV of flexible structures. By a simple analytical development on the stability of an infinite cable/wake system, we demonstrate the existence a temporal instability. The theoretical study is pushed further to finite structure, a tensioned cable, for which modes frequency, amplitude growth rate in time and velocity range of instability are easily derived. The developed concepts are used to explain experimentally observed behaviours of a low flexural rigidity tensioned beam undergoing VIV.

NOMENCLATURE

Dimensional

C, D, F_Y Phase velocity (m/s), diameter (m), fluid force (N/m)
T, U Time (s), flow velocity (m/s)
V_Y Structure displacement eigenvector (m)
Y, Z Structure displacement (m), spanwise position (m)
f, m_S, r_S Movement frequency (Hz), structure linear density (kg/m), structure damping (N s/m^2)
ρ, Θ Fluid density (kg/m^3), tension (N)

Dimensionless

A, M Structure/wake coupling parameters
V_Q Wake eigenvector
C_{L_0} Fluctuating lift coefficient for a fixed cylinder
C_D Mean sectional drag coefficient
C_{M_0} Potential added mass coefficient in still fluid
S_T Strouhal number
k, n Wave number, mode number
t, u Time, reduced velocity
y, z Structure displacement, spanwise position
$\hat{q}$, $\hat{y}$ Wake variable amplitude, structure mouvement amplitude,
σ, γ, μ Structure damping coefficient, stall parameter, mass number
Λ, ω, ε Structure aspect ratio, complex frequency, phenomenological parameter

INTRODUCTION

Vortex-induced vibration (VIV) of risers is a subject of high concern as drilling and production operations move into ever deeper waters. When lock-in occurs, i.e. when the frequency of the vortex shedding synchronizes with the structure vibration frequency, the amplitude of movement is of the order of the diameter of the bluff body, leading to fatigue damage. For flexible structures, fatigue damage goes with frequency and bending stress, the later being related to the vibration wave length or vibration mode. It is thus important to predict which mode of vibration will lock-in with the wake. Despite the fact that a large body of literature is available on the understanding and the prediction of lock-in range for single degree of freedom rigid structures, the behaviour of slender structures under uniform current

*Address all correspondence to this author.

is yet not fully understood.

In a recent paper, de Langre [1] showed that the lock-in mechanism can be interpreted as a linear instability caused by the merging of the two eigenfrequencies of a dynamic system that includes two coupled oscillators, namely the wake and the structure. This instability is also referred to as coupled mode flutter [2]. His study was performed using a linearised version of the wake oscillator model described in [3]. Following the work of de Langre, a simple theory based on a linear stability analysis is used here to explains some aspects of VIV of flexible structures subjected to uniform flows such as individual mode lock-in range definition and the occurrence of "mode switching" as define by Chaplin *et al.* in [4]. The terminology "time sharing" is also used for this phenomenon, [5].

This paper is separated in three parts. First the linear wake oscillator model is explained for a tension cable. Second, the instability mechanism and its characteristics are studied. Third, comparisons are made between results of the linear model and experimental results by Chaplin *et al.* [4].

MODEL DESCRIPTION

A linear version of the wake oscillator model for a tension cable described in [6] is used here. Considering only the cross flow displacement of the cable, $Y(Z,T)$, the dynamic equation can be written as

$$m_S\frac{\partial^2 Y}{\partial T^2}+r_S\frac{\partial Y}{\partial T}-\Theta\frac{\partial^2 Y}{\partial Z^2}=F_Y, \tag{1}$$

with

$$F_Y=\frac{1}{4}\rho U^2 D C_{L_0} q-\frac{\pi}{4}\rho D^2 C_{M_0}\frac{\partial^2 Y}{\partial T^2}-\frac{1}{2}\rho D C_D U\frac{\partial Y}{\partial T}. \tag{2}$$

In the equation above, C_{L_0} is the fluctuating lift coefficient for a fixed rigid cylinder, C_D is the mean sectional drag coefficient, $C_{M_0}=1$ is the potential added mass coefficient in still fluid, ρ is the fluid density, U is the flow velocity, D the structure diameter, Θ the tension, r_S the structural damping and m_S the linear density of the cable. Following [7], the dynamic of the local fluctuating lift coefficient, $q(Z,T)$, is modelled using the distributed wake oscillator

$$\frac{\partial^2 q}{\partial T^2}-\varepsilon\left(2\pi S_T\frac{U}{D}\right)\frac{\partial q}{\partial T}+\left(2\pi S_T\frac{U}{D}\right)^2 q=A\frac{\partial^2 Y}{\partial T^2}, \tag{3}$$

where S_T is the Strouhal number and $A=12$ and $\varepsilon=0.3$ are empirical constant (see [3]).

The system studied composed by the Eqs. (1) and (3) is studied here considering the wake and the structure as a unique medium in which vibration waves travel. Those waves have two components, the cable displacement $Y(Z,T)$ and the fluctuating lift $Y(Z,T)$. Figure 1 illustrates this concept.

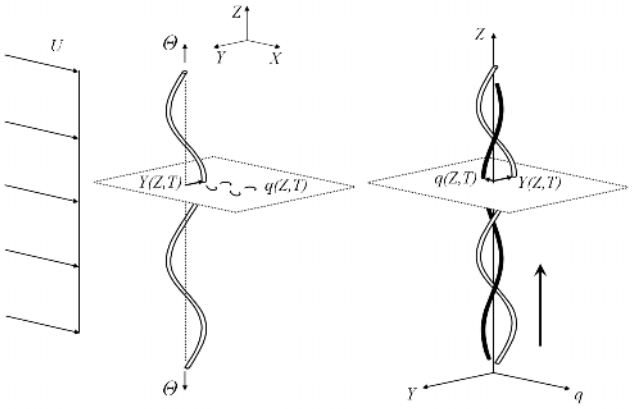

Figure 1 It is proposed here to consider the wake and the structure as one unique medium (right figure) representing two distinct elements interacting (left figure).

Using the cable diameter D and its undamped phase velocity C defined as

$$C=\sqrt{\frac{\Theta}{m_S+\frac{\pi}{4}\rho D^2}}, \tag{4}$$

for reference length and time, one can write the dimensionless equations of the model

$$\frac{\partial^2 y}{\partial t^2}+\left(\sigma+\frac{\gamma}{\mu}u\right)\frac{\partial y}{\partial t}-\frac{\partial^2 y}{\partial z^2}=Mu^2 q, \tag{5}$$

$$\frac{\partial^2 q}{\partial t^2}-\varepsilon u\frac{\partial q}{\partial t}+u^2 q=A\frac{\partial^2 y}{\partial t^2}, \tag{6}$$

with $z=Z/D$, $y=Y/D$ and $t=(C/D)T$. The new parameters in the above equations read

$$\sigma=\left(\frac{D}{m_T C}\right)r_S, \qquad u=2\pi S_T\frac{U}{C}$$
$$\gamma=\frac{C_D}{4\pi S_T}, \qquad M=\frac{C_{L_0}}{16\pi^2 S_T^2\mu}. \tag{7}$$

As shown by Facchinetti *et al.* in [3], the coefficient M is a mass number that scales the effect of the wake on the structure, and γ is the stall parameter. The dimensionless velocity u is referred to here as the reduced velocity.

In order to derive simple analytical solutions for the cable/wake system, the damping terms in Eqs. (5) and (6) are disregarded. Note that de Langre in [1] has shown that the damping terms do not change the instability mechanism in the case of an elastically supported rigid cylinder. The simplified system therefore reads

$$\frac{\partial^2 y}{\partial t^2} - \frac{\partial^2 y}{\partial z^2} = M u^2 q, \tag{8}$$

$$\frac{\partial^2 q}{\partial t^2} + u^2 q = A \frac{\partial^2 y}{\partial t^2}. \tag{9}$$

1 LINEAR STABILITY APPROACH

1.1 Instability mechanism

Solutions in the form of propagating waves are searched here

$$\begin{bmatrix} y(z,t) \\ q(z,t) \end{bmatrix} = \begin{bmatrix} \hat{y} \\ \hat{q} \end{bmatrix} e^{i(\omega t + kz)}, \tag{10}$$

where ω is the frequency, k the wave number and $\hat{y}$ and $\hat{q}$ the complex amplitude of the structural and the wake part of waves respectively. Inserting this form of solution into Eqs. (8) and (9), one finds the dispersion relation of the cable/wake medium

$$\mathcal{D}(\omega, k; u) = \omega^4 + [(AM-1)u^2 - k^2]\omega^2 + k^2 u^2 = 0. \tag{11}$$

It should be noted that the dispersion relation combines the coupling terms A and M into a single parameter, AM. Using Eq.(11), we can study the stability of the cable/wake system. Writing ω as a function of k and u, one obtains

$$\omega(k,u) = \pm\frac{1}{2}\left[\alpha \pm \sqrt{\alpha^2 - 4k^2u^2}\right]^{1/2}, \tag{12}$$

with $\alpha = k^2 + (1-AM)u^2$. Equation (12) shows that there are four frequencies for each reduced velocity. They come by pairs of opposite signs meaning that the waves with the same frequency propagate in opposite directions. Moreover, one can remark that ω is complex when

$$-2ku < \alpha < 2ku \tag{13}$$

Using this inequality we can define for a fixed wave number the range of reduced velocities for which we have a complex frequency

$$\frac{k}{1+\sqrt{AM}} < u < \frac{k}{1-\sqrt{AM}}. \tag{14}$$

In this range of u, the real and imaginary parts of the dimensionless frequency are

$$\mathrm{Re}[\omega] = \frac{1}{2}\sqrt{k^2 + 2uk + (1-AM)u^2}, \tag{15}$$

$$\mathrm{Im}[\omega] = \pm\frac{1}{2}\sqrt{-k^2 + 2uk + (AM-1)u^2}. \tag{16}$$

Figure 2 shows the typical evolution of ω with u for a given wave number k. At low and high reduced velocity, two neutral waves exist. The two waves have their frequency merging for a certain range of u leading to complex conjugates ω. In this range, the system is characterised by an unstable wave (growing in amplitude with time) and a damped wave (decreasing in amplitude with time). A temporal instability has thus been identified for the cable/wake system. This instability is in time and is coming from the confusion of the frequency of two propagating waves. Equation (14) defines the reduced velocity range for which this instability occurs (for a given wave number) and Eqs. (15) and (16) give the complex frequency ($\mathrm{Re}[\omega]$) and the growth rate ($-\mathrm{Im}[\omega]$).

1.2 Mode instability range

A finite tensioned cable of aspect ratio $\Lambda = L/D$ and exposed to a uniform flow is now considered, Figure 3. The extremities of this cable are fixed, so that the boundary conditions for the structure are

$$y(0,t) = 0, \qquad y(\Lambda,t) = 0. \tag{17}$$

No condition for the wake variable is necessary since there is no spanwise interaction for q. Solutions with real wave numbers are still searched for here. Considering the end conditions from Eq. (17), the allowable wave numbers are

$$k_n = \frac{\pi}{\Lambda} n, \tag{18}$$

with $n = 1, 2, 3 \ldots$. The terminology of mode number is applicable here to the parameter n. The interest now is to characterise the stability of the system in the range of reduced velocities where Mode n is unstable. Rewriting Eq. (14), Mode n is unstable for reduced velocities u that satisfy

$$\left(\frac{\pi}{\Lambda}\right)\frac{n}{1+\sqrt{AM}} < u < \left(\frac{\pi}{\Lambda}\right)\frac{n}{1-\sqrt{AM}}. \tag{19}$$

In this range of reduced velocities, the real and imaginary parts of the dimensionless frequency (from Eqs. 15 and 16) are

$$\mathrm{Re}[\omega] = \left(\frac{\pi}{2\Lambda}\right)\sqrt{n^2 + 2n\beta + (1-AM)\beta^2}, \tag{20}$$

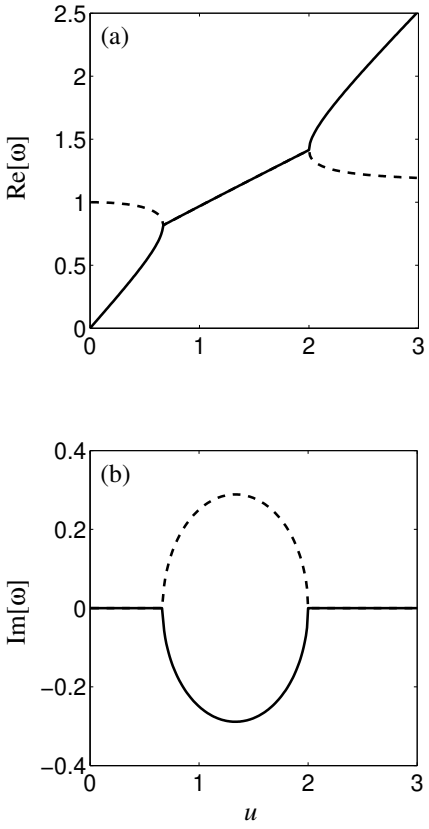

Figure 2 Complex frequency ω evolution with *u* for *k=1* and *AM=0.25*: (a) Re[ω], (b) Im[ω].

$$\mathrm{Im}[\omega] = -\left(\frac{\pi}{2\Lambda}\right)\sqrt{-n^2+2n\beta+(AM-1)\beta^2}, \qquad (21)$$

with $\beta = (\Lambda/\pi)u$. Figure 4 shows the real and imaginary part of ω for Mode 2 and 3 and for two values of *AM*. One can see that the evolution of Re[ω] of each mode is close to linear. Also, the real part of the frequency is discontinuous from one mode to the other giving a stairs like form of evolution with the reduced frequency. This type of vibration frequency evolution with flow velocity is reported in [8] for a tensioned cable and in [4] for a low flexural rigidity tensioned beam. As seen in Fig. 4 (b and d), the modes growth rate curves (-Im[ω]) go through a maximum value in the middle of the range of reduced velocities defined by Eq. (14)

$$u_{max} = \left(\frac{\pi}{\Lambda}\right)\left(\frac{n}{1-AM}\right), \qquad (22)$$

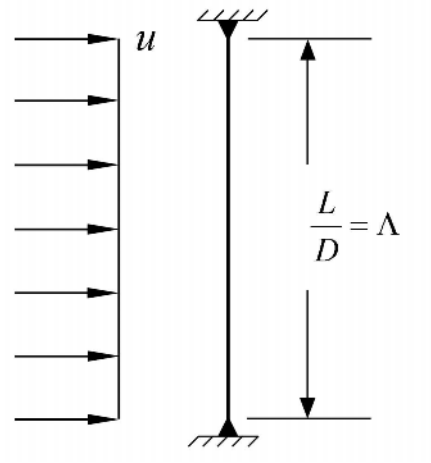

Figure 3 Tensioned cable under uniform flow. Extremities are fixed.

where the corresponding growth rate is

$$-\mathrm{Im}[\omega_{max}] = \left(\frac{\pi}{2\Lambda}\right) n\sqrt{\frac{AM}{1-AM}}. \qquad (23)$$

The maximum growth rate, an thus the fastest pace at which a given mode amplitude will grow in time, increases with *n* and *AM*. Finally, one can also note that the ranges of unstable reduced velocities of different modes can overlap. This important result means that for one reduced velocity, more than one mode can be unstable.

COMPARISONS WITH EXPERIMENTAL RESULTS

Lock-in mode transition

In the previous section, it has been shown that for a finite cable in uniform flow, there are possible overlaps of unstable reduced velocities ranges of two (or more) adjacent modes. One can make the assumption that the most instable one would be seen in practice since its amplitude grows faster in time. This assumption is validated here by comparison between results from the linear theory and experiments by Chaplin *et al.* in [4].

A sketch of their experiment setup is shown on Figure 5. It consists of a tensioned beam of low flexural rigidity subjected to a uniform flow on nearly half of its length, the other part being in stagnant water. Table 1 shows the mechanical characteristics of the structure. The tension specified is the one measured at the top of the structure. The Reynolds number of the test ranged from 2500 to 25000. The flow is generated by carrying the assembly in the stagnant water of a flume. The structure is thus mounted on a cabin moving on rails.

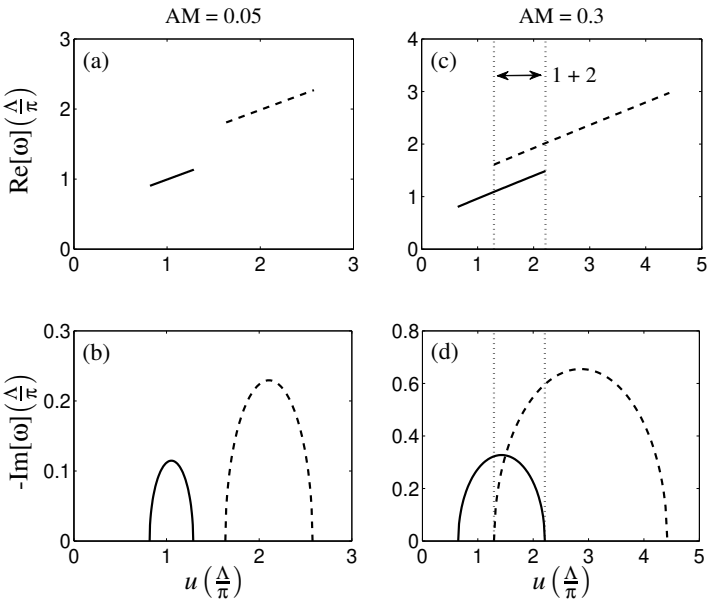

Figure 4 Dimensionless frequency for Mode 1 (solid line) and 2 (dashed line) for a tensioned cable with fixed extremities at *AM* = 0.05: real part (a) and imaginary part (b), and at *AM* = 0.3: real part (c) and imaginary part (d). Dotted lines indicate the limits of the region where the two modes are unstable.

Properties	Value	Properties	Values
L (m)	13.12	Θ (N)	1925
D (m)	0.028	EI (Nm^2)	29.1
m_S (kg/m)	1.8	$\partial\Theta/\partial Z$	12.1

Table 1 Mechanical properties of the structure in [4].

In [4], the authors describe the response of the structure by

$$Y(Z,T) = \sum_n Y_n(T)\ sin\left(\frac{n\pi Z}{L}\right) \tag{24}$$

where n is the mode number and $Y_n(T)$ is the modal weight computed from the experiment. Figure 6 (a) shows the dominant mode at five different velocities. One can note that the low velocities are dominated by Mode 2 while the highest by Mode 3.

The structure is modeled here using the equation of an Euler beam with variable tension

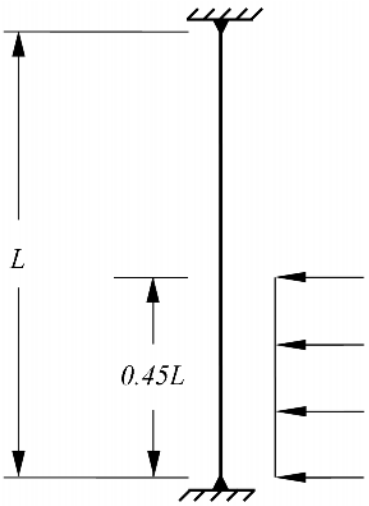

Figure 5 Schematic of the experimental setup used by Chaplin *et al.* in [4].

$$m_S\frac{\partial^2 Y}{\partial T^2} - \frac{\partial}{\partial Z}\left(\Theta\frac{\partial Y}{\partial Z}\right) + EI\frac{\partial^4 Y}{\partial Z^4} = F_Y. \tag{25}$$

The expression of the fluid force F_Y is recalled here

$$F_Y = \frac{1}{4}\rho U^2 D C_{L_0} q - \frac{\pi}{4}\rho D^2 C_{M_0}\frac{\partial^2 Y}{\partial T^2} - \frac{1}{2}\rho D C_D U\frac{\partial Y}{\partial T},$$

with the wake variable q dynamics still being defined by Eq. (3). A numerical modal analysis is used to study the linear system defined by Eqs. (2), (3) and (25). In order to do so, the derivatives with regards to the spanwise coordinate Z are approximated using the centered finite difference method of order 2. The structure/wake medium is thus discretised in a number of coupled oscillators. The dynamic system obtained is written

$$\begin{bmatrix} \mathcal{M}_S & \mathcal{M}_{FS} \\ \mathcal{M}_{SF} & \mathcal{M}_F \end{bmatrix}\begin{pmatrix} \ddot{\mathcal{Y}} \\ \ddot{\mathcal{Q}} \end{pmatrix} + \begin{bmatrix} \mathcal{R}_S & \mathcal{R}_{FS} \\ \mathcal{R}_{SF} & \mathcal{R}_F \end{bmatrix}\begin{pmatrix} \dot{\mathcal{Y}} \\ \dot{\mathcal{Q}} \end{pmatrix} + \\ + \begin{bmatrix} \mathcal{K}_S & \mathcal{K}_{FS} \\ \mathcal{K}_{SF} & \mathcal{K}_F \end{bmatrix}\begin{pmatrix} \mathcal{Y} \\ \mathcal{Q} \end{pmatrix} = 0 \tag{26}$$

where $\mathcal{Y} = [Y_1(T)\ \cdots\ Y_j(T)]^T$ and $\mathcal{Q} = [q_1(T)\ \cdots\ q_r(T)]^T$, r being the number of discretisation points in the flow zone.

The form of solutions search for reads

$$\begin{pmatrix} \mathcal{Y} \\ \mathcal{Q} \end{pmatrix} = \begin{pmatrix} V_Y \\ V_Q \end{pmatrix} e^{i\omega' T}, \tag{27}$$

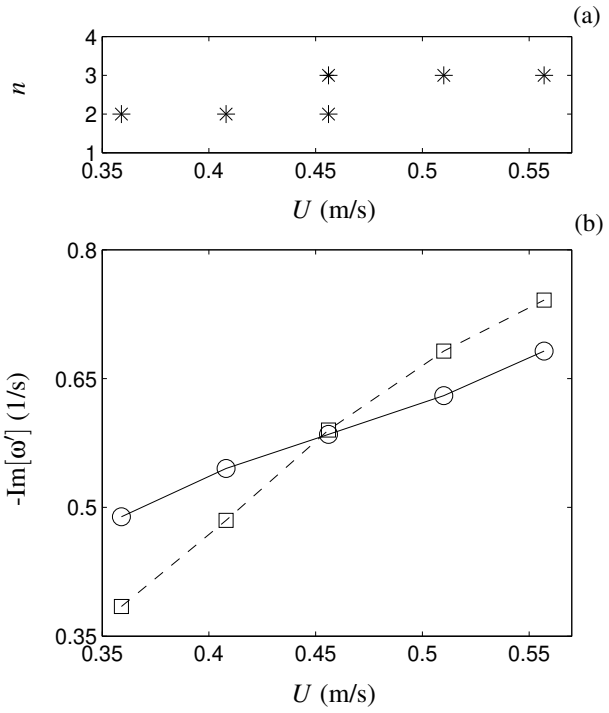

Figure 6 Comparison between experiments and linear theory for dominant mode: (a) experimental results reported by Chaplin *et al.* in [4], (b) growth rates of Mode 2 (circles) and Mode 3 (squares).

where ω' is the dimensional frequency and V_Y and V_Q are the eigenvectors of the structure displacement and the wake variable respectively. Boundary conditions imposed are

$$\frac{\partial^2 Y}{\partial Z^2}(0,T) = \frac{\partial^2 Y}{\partial Z^2}(L,T) = 0,$$
$$Y(0,T) = Y(L,T) = 0. \tag{28}$$

Since no analytical development is done here, the damping terms are kept. For the range of Reynolds number considered, $C_{L_0} = 0.2$, [9]. Also, a C_D of 2 and S_T of 0.17 are used following measurements of those quantities by Chaplin *et al.* in [4].

The numerical modal calculation gives complex eigenvectors V_Y and V_Q, meaning modes in form of a travelling wave. For the flow velocities discussed above, Figure 7 shows V_Y of the two most unstable modes. The shapes are similar to those defined by Eq. (24) for $n = 2$ and $n = 3$. The dimensional growth rates predicted by the linear model for Mode 2 and 3 are shown on Fig. 6 (b). One can observe that linear Mode 2 has the highest growth rate for the lowest velocities. For $U = 0.46m/s$, the growth rates of both modes are equal and Mode 3 has the highest growth rate for the last two velocities. As seen on Fig. 6, this mode transition

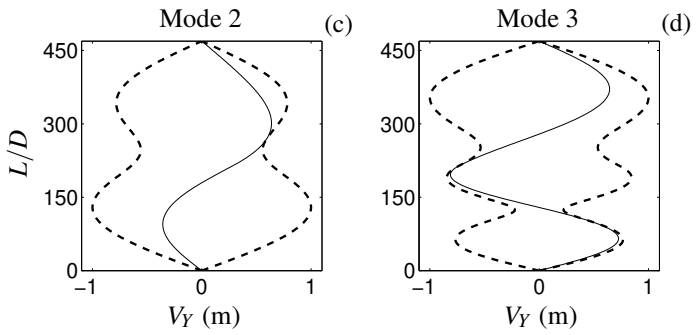

Figure 7 Linear model prediction for the spatial shape of Mode 2 and 3 for the structure, $|V_Y|$ (dashed line) and Re[V_Y] (solid line)

compares well with the experimental measurements. The situation at $U = 0.46m/s$ represents, as reported in [4], a particular case where the modal weights exhibit considerable modulations in time. This phenomenon is studied in the next section.

Time sharing

Chaplin *et al.* in [4] detail cases of what they refer to as "mode switching". They report that this mode switching was triggered by disturbances like vibrations in the carriage system due to irregularities in the rails. Figure 8 shows an example of this phenomenon. From this figure, it is clear that two regimes dominate the system response at different time. The first regime of the response (called here Regime A) is dominated by Mode 8. The second regime (called here Regime B) is a mixture of Modes 6 and 7. Note that Mode 4 and 5 participate also to the response. They are not shown here for the sake of clarity. The temporal response of the structure is shown for both regimes on Figure 9. This figure shows as well the displacement of the structure at a given time.

For this configuration, the linear modal calculation predicts two modes with equal growth rates that are associated here to Regime A and Regime B respectively. The shape of those linear modes is compared to the response of the structure on Fig. 9. One can see that the predicted wave length for both modes is close to the ones obtained experimentally. The evolution of the pseudo frequency with time (obtained by wavelets analysis of the modal weights) is shown on Fig. 8 (d) for Modes 6 and 7 and (e) for Mode 8. The pseudo frequency evolution is obtained by taking the frequency with maximum coefficient over one period of motion. This pseudo frequency is then averaged on ten periods of vibration. From this figure, it is clear that two frequencies dominate the structure response at different time. The two frequencies "share" the time of the response, owing the name "time sharing" here and in [5]. Note that this phenomenon occurs also in the case of non uniform flows as experimentally demonstrated

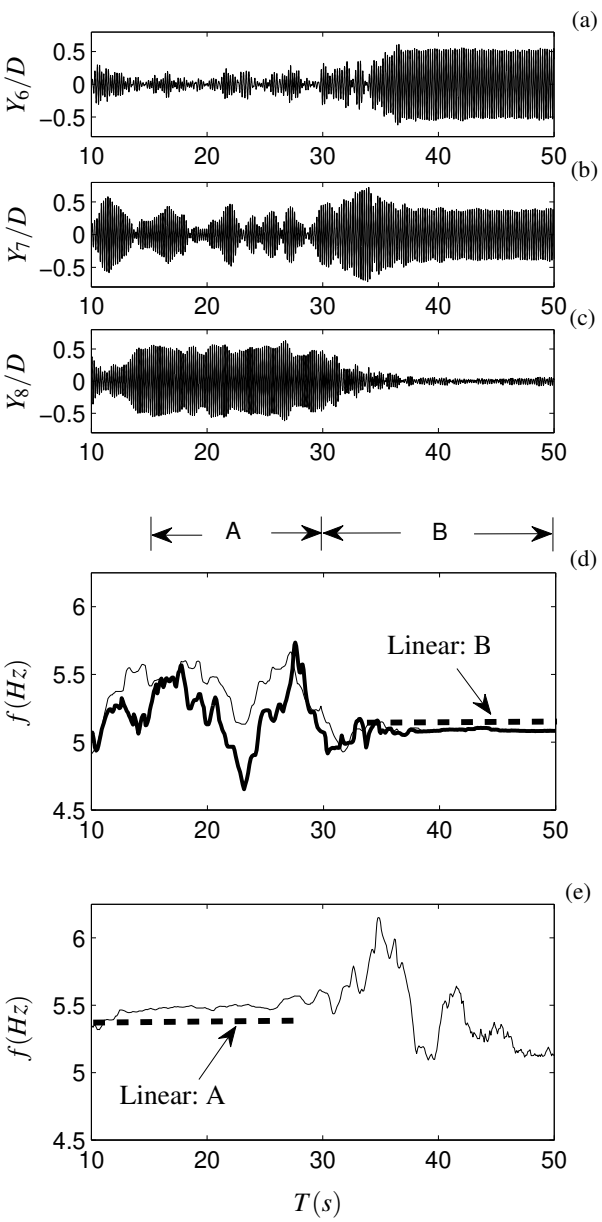

Figure 8 (a)-(c) Time evolution of the modal weight of Mode 6 to 8, (d) pseudo frequency evolution with time of Mode 7 (thin line) and Mode 6 (solid line), (e) pseudo frequency evolution with time for modal weight of Mode 8. On (d) and (e), the linear theory prediction for frequencies is shown with dashed lines. Experiments by Chaplin *et al.* [4]. Top tension is $\Theta = 1073$ N and flow velocity is $U = 0.9$ m/s.

in [5].

Results presented here indicate that time sharing is a consequence to the fact that two (or more) modes are equally unstable, and thus growing in time at the same pace making the system

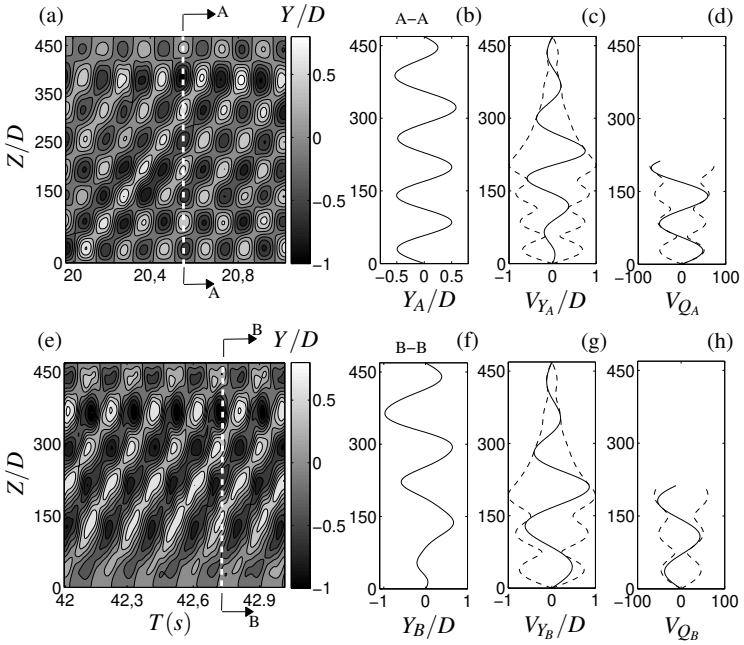

Figure 9 Regime A (first line): (a) Evolution with time and space of structure displacement in experiment, (b) instantaneous displacement of the structure, (c) linear theory prediction of the modal shape for the structure, (d) linear theory prediction of the modal shape for the wake. Second line: idem for Regime B. Experiments by Chaplin *et al.* [4].

sensible to perturbations, vibrations in the experimental apparatus in this case. The effect of vibration perturbations on lock-in is discussed in [10].

CONCLUSION

In this paper, a linearized version of the wake oscillator model developed by Facchinetti *et al.* in [6] was used to understand VIV of long flexible structures. After a description of this linear model, a simple analytical development on the stability of the cable/wake system has shown that a temporal instability occurs for a given wave number over a range of reduced velocities. This instability comes from the merging of the frequencies of two different waves propagating in the system. This concept was then applied to a finite cable/wake medium for which the instability range, the frequencies and the growth rates of the different modes was found. It was also noted that more than one mode could be unstable at a given reduced velocity. The assumption was thus made that the most unstable mode would be the one observed in the non linear steady state response of the system. This assumption was then validated against experimental results by Chaplin *et al.* in [4] on a tensioned beam of low flexural rigidity. Using a numerical modal calculation, it was found that the lin-

ear model predicted the transition from one mode lock-in range to another. Thus, the linear growth rates of the different mode can be related to the steady state response of the structure undergoing VIV. Also, it was found that "time sharing", or "mode switching" is symptomatic to the fact that two or more modes have very similar growth rates.

ACKNOWLEDGMENT

The authors would like to express their gratitude to Prof. J.R. Chaplin for providing the data from experiments.

REFERENCES

[1] de Langre, E., 2006. "Frequency lock-in is caused by coupled-mode flutter". *Journal of Fluids and Structures,* **22**(6-7), Oct., pp. 783–791.

[2] Blevins, R., 1990. *Flow-Induced Vibration*. Van Nostran Reinhold, New York.

[3] Facchinetti, M., de Langre, E., and Biolley, F., 2004. "Coupling of structure and wake oscillators in vortex-induced vibrations". *Journal of Fluids And Structures,* **19**(2), Feb., pp. 123–140.

[4] Chaplin, J., Bearman, P., Huarte, F. H., and Pattenden, R., 2005. "Laboratory measurements of vortex-induced vibrations of a vertical tension riser in a stepped current". *Journal of Fluids and Structures,* **21**(1), Nov., pp. 3–24.

[5] Swithenbank, S., 2007. "Dynamics of long flexible cylinders at high-mode number in uniform and sheared flows". PhD thesis, Massachusetts Institute of Technology.

[6] Facchinetti, M., de Langre, E., and Biolley, F., 2004. "Vortex-induced travelling waves along a cable". *European Journal of Mechanics B-Fluids,* **23**(1), Feb., pp. 199–208.

[7] Mathelin, L., and de Langre, E., 2005. "Vortex-induced vibrations and waves under shear flow with a wake oscillator model". *European Journal of Mechanics B-Fluids,* **24**(4), Aug., pp. 478–490.

[8] King, R., 1995. "An investigation of vortex induced vibrations of sub-sea communications cables". In Proceedings of the Sixth International Conference on Flow Induced Vibration, Bearman P.W., pp. 443–454.

[9] Norberg, C., 2003. "Fluctuating lift on a circular cylinder: review and new measurements". *Journal of Fluids and Structures,* **17**(1), pp. 57–96.

[10] Vandiver, J., 1993. "Dimensionless parameters important to the prediction of vortex-induced vibration of long, flexible cylinders in ocean currents". *Journal of Fluids and Structures,* **7**(5), July, pp. 423–455.